DE-Vol. 32-2, Advances in Design Automation – Vol. 2
ASME 1991

THE FORMULATION OF KINEMATIC CONSTRAINTS IN DESIGN-ORIENTED MACHINE DYNAMICS

Subir Kumar Saha and Jorge Angeles
Department of Mechanical Engineering
McGill Research Centre for Intelligent Machines
McGill University
Montreal, Quebec, Canada

Abstract

In the realm of the dynamic analysis of machinery for design purposes, the determination of non-working constraint forces, which do not appear in simulation studies, is of the utmost importance. The said forces can be readily computed if suitable kinematic constraints are available. In this paper, a formulation of kinematic constraints is adopted, that pertains to the *natural orthogonal complement* method, introduced elsewhere, for the dynamic modeling of mechanical systems. This formulation is illustrated with several examples.

1 Introduction

Mechanical systems arising in machinery are usually subjected to kinematic constraints that limit the motion capabilities of the individual machine elements. These constraints can be expressed algebraically by a set of constraint equations, which can take on a variety of forms. These forms depend largely on the choice of the formulation method. For example, in modeling holonomic systems with either the Newton-Euler or the Euler-Lagrange methods (Meirovitch, 1970), constraint equations in the form of—usually nonlinear—functions of the generalized coordinates are established. Alternatively, for example, as proposed by Kane and Wang (1965) and Huston and Passerello (1974), constraints can be expressed as linear, although not necessarily homogeneous, equations in the generalized velocities.

Within the framework of the methodology termed *the natural orthogonal complement* (Angeles and Lee, 1988), both holonomic and nonholonomic constraints are expressed as a system of equations that are *linear and homogeneous* in the *twists* of all the bodies of the system. Here, we understand as the twist of a body a 6-dimensional vector containing the necessary and sufficient information determining the velocity field throughout the body. It thus contains the three components of the angular velocity vector and the three components of the velocity of the mass center, although any other point of the body could be used. The aforementioned methodology was originally proposed for holonomic systems, but it was later extended to nonholonomic systems (Saha and Angeles, 1991). It has also been successfully used for the simulation of n-axis serial robotic manipulators (Angeles and Ma, 1988), flexible-link manipulators (Cyril, Angeles and Misra, 1989) and automatic guided vehicles (Saha and Angeles, 1989). The crucial step in successfully modeling a broad class of mechanical systems with the natural orthogonal complement is the representation of the kinematic constraints. We illustrate this formulation as applied to several mechanical systems. Moreover, dynamics models of these systems are obtained using this method.

2 Kinematic Constraints

First, the *twist* $\mathbf{t}_i$ of the ith rigid link of the machine at hand, undergoing an arbitrary motion in the three-dimensional space, is defined in terms of its angular velocity, $\boldsymbol{\omega}_i$, and the velocity of the corresponding mass center, $\dot{\mathbf{c}}_i$, both being, in general, three-dimensional vectors. Hence,

$$\mathbf{t}_i \equiv \begin{bmatrix} \boldsymbol{\omega}_i \\ \dot{\mathbf{c}}_i \end{bmatrix}$$

Moreover, we assume that the ith body of the system under study, comprising l rigid links and k kinematic pairs, is coupled to the jth link through either a holonomic or a nonholonomic coupling. Thus, the coupling of this link with the jth link is represented as a linear homogeneous equation in the twists of the two coupled links, namely,

$$\mathbf{A}_{i,i}\mathbf{t}_i + \mathbf{A}_{i,j}\mathbf{t}_j = \mathbf{0}, \quad \text{for } i = 1, \cdots, k;\ i, j \in [1, l] \text{ and } i \neq j \quad (1)$$

Thus, for q scalar constraints, the $q \times 6$ coefficient matrices $\mathbf{A}_{i,i}$ and $\mathbf{A}_{i,j}$ are, in general, configuration-dependent. Furthermore, a holonomic coupling produces six scalar, linearly dependent constraints, whereas a nonholonomic coupling produces three independent scalar constraints (Saha and Angeles, 1991).

3 Modeling Technique

The method of *the natural orthogonal complement*, introduced in Angeles and Lee (1988) and based on the kinematic formulation outlined in Section 2, is described briefly. Some vectors and matrices, used to derive the equations of motion of a system consisting of l links, are defined below:

$\mathbf{w}_i$: the *wrench* acting on the ith link. It is defined, in accordance with the definition of $\mathbf{t}_i$, as

$$\mathbf{w}_i \equiv \begin{bmatrix} \mathbf{n}_i \\ \mathbf{f}_i \end{bmatrix}$$

where $\mathbf{n}_i$ and $\mathbf{f}_i$ denote the resultant torque and the resultant force acting at the mass center of the ith link, respectively.

Ω_i: the *cross-product* matrix associated with vector ω_i. It is defined as

$$\Omega_i \equiv \frac{\partial(\omega_i \times \mathbf{x})}{\partial \mathbf{x}} \equiv \omega_i \times \mathbf{1} \tag{2}$$

for an arbitrary 3-dimensional vector $\mathbf{x}$. Henceforth, the *cross-product* matrix of any 3-dimensional vector $\mathbf{v}$ will be denoted by $\mathbf{V}$, unless otherwise indicated.

$\mathbf{W}_i$ & $\mathbf{M}_i$: 6×6 matrices of *extended angular velocity*, and of *extended mass*, respectively. These are

$$\mathbf{W}_i \equiv \begin{bmatrix} \Omega_i & \mathbf{O} \\ \mathbf{O} & \mathbf{O} \end{bmatrix}, \qquad \mathbf{M}_i \equiv \begin{bmatrix} \mathbf{I}_i & \mathbf{O} \\ \mathbf{O} & m_i\mathbf{1} \end{bmatrix} \tag{3}$$

where m_i, $\mathbf{I}_i$, $\mathbf{O}$ and $\mathbf{1}$ denote the mass, the inertia matrix of the ith link about its mass center, the zero and the identity 3×3 matrices, respectively.

θ: p-dimensional vector of *generalized coordinates*, not necessarily independent in general, where $p = n + m$, n being the degree of freedom of the machine. Thus, n is equal to the number of elements in the minimal set of generalized coordinates. Furthermore, in the absence of redundant actuation, n equals also the number of *actuated* joints, whereas m is the number of dependent coordinates or *unactuated* joints.

$\mathbf{t}$ & $\mathbf{w}$: $6l$-dimensional vectors of *generalized twist* and *generalized wrench*, respectively, i.e.,

$$\mathbf{t} \equiv \begin{bmatrix} \mathbf{t}_1 \\ \mathbf{t}_2 \\ \vdots \\ \mathbf{t}_l \end{bmatrix}, \qquad \mathbf{w} \equiv \begin{bmatrix} \mathbf{w}_1 \\ \mathbf{w}_2 \\ \vdots \\ \mathbf{w}_l \end{bmatrix}$$

$\mathbf{W}$ & $\mathbf{M}$: $6l \times 6l$ matrices of *generalized angular velocity* and *generalized mass*, respectively, namely,

$$\begin{aligned} \mathbf{M} &\equiv \mathrm{diag}[\mathbf{M}_1, \mathbf{M}_2, \ldots, \mathbf{M}_l] \\ \mathbf{W} &\equiv \mathrm{diag}[\mathbf{W}_1, \mathbf{W}_2, \ldots, \mathbf{W}_l] \end{aligned}$$

Now, if all vectors and matrices associated with the ith link are referred to a coordinate system fixed to the link, then the Newton–Euler equations governing the motion of this link can be written as

$$\mathbf{M}_i\dot{\mathbf{t}}_i = -\mathbf{W}_i\mathbf{M}_i\mathbf{t}_i + \mathbf{w}_i, \quad i = 1, \cdots, l \tag{4}$$

Therefore, if the machine under study comprises l links, $6l$ uncoupled Newton–Euler equations are derived. These take the form

$$\mathbf{M}\dot{\mathbf{t}} = -\mathbf{W}\mathbf{M}\mathbf{t} + \mathbf{w}^W + \mathbf{w}^N \tag{5}$$

Moreover, $\mathbf{w}^W$ and $\mathbf{w}^N$ are the *working* and the *nonworking* generalized constraint wrenches, respectively, such that

$$\mathbf{w} = \mathbf{w}^W + \mathbf{w}^N$$

Next, with the methodology developed in the previous section, the kinematic constraints produced by γ holonomic and ν nonholonomic couplings can be written, from eq.(1), as

$$\mathbf{A}\mathbf{t} = \mathbf{0} \tag{6}$$

where $\mathbf{A}$ is a $(6\gamma+3\nu)\times 6l$ matrix that is termed here the *kinematic constraint matrix*. Moreover, the vector of generalized twist can be represented as a linear transformation of vector $\dot{\theta}$, namely,

$$\mathbf{t} = \mathbf{T}\dot{\theta} \tag{7}$$

where $\mathbf{T}$ is a $6l \times p$ matrix. Upon substitution of $\mathbf{t}$ into eq.(6), we obtain

$$\mathbf{A}\mathbf{T}\dot{\theta} = \mathbf{0} \tag{8}$$

If all the components of vector $\dot{\theta}$ are *independent*, i.e., if $p = n$ and $m = 0$, then, from eq.(8), the relation shown below is readily obtained:

$$\mathbf{A}\mathbf{T} = \mathbf{0} \tag{9}$$

where the $6l \times n$ matrix $\mathbf{T}$ is called *the natural orthogonal complement* (Angeles and Lee, 1988) of $\mathbf{A}$. By virtue of the definition of $\mathbf{A}$ and the vector of nonworking constraint wrenches, the latter turns out to lie in the range of the transpose of $\mathbf{A}$ and hence, the said wrench lies in the nullspace of the transpose of $\mathbf{T}$. Therefore, upon multiplication of both sides of the $6l$-dimensional Newton–Euler uncoupled equations of the system, eq.(5), by the transpose of $\mathbf{T}$, the vector of nonworking constraint wrenches is eliminated from the said equation. Moreover, $\dot{\mathbf{t}}$ is obtained by differentiating eq.(7) as

$$\dot{\mathbf{t}} = \mathbf{T}\ddot{\theta} + \dot{\mathbf{T}}\dot{\theta} \tag{10}$$

Hence, the n independent constrained dynamical equations of motion are derived as

$$\mathbf{I}(\theta)\ddot{\theta} = \mathbf{C}(\theta, \dot{\theta})\dot{\theta} + \tau \tag{11}$$

where

$\mathbf{I}(\theta) \equiv \mathbf{T}^T\mathbf{M}\mathbf{T}$: $n \times n$ matrix of generalized inertia,

$\mathbf{C}(\theta, \dot{\theta}) \equiv -\mathbf{T}^T(\mathbf{W}\mathbf{M}\mathbf{T} + \mathbf{M}\dot{\mathbf{T}})$: $n \times n$ matrix of convective inertia terms,

$\tau \equiv \mathbf{T}^T\mathbf{w}^W$: n-dimensional vector of generalized external force arising from actuation, gravity and dissipation effects.

Note that, if the components of vector $\dot{\theta}$ are not independent, i.e., if $m \neq 0$, the expression in eq.(9) cannot be obtained from eq.(8), and hence, matrix $\mathbf{T}$, as in eq.(7), in the presence of dependent or *unactuated* joints is not the natural orthogonal complement of $\mathbf{A}$. In order to use this method for the dynamic analysis of mechanisms with multiple kinematic loops, matrix $\mathbf{T}$ is obtained as follows: an $m' \times p$ matrix $\mathbf{J}$, the Jacobian matrix, is introduced, whose rows are the m' independent rows of matrix $\mathbf{AT}$, these independent constraint equations being represented as

$$\mathbf{J}\dot{\theta} = \mathbf{0} \tag{12}$$

Note that it is not recommended to compute matrix $\mathbf{J}$ from eq.(8). In fact, it can be efficiently obtained using the independent loop equations of the whole kinematic chain (Gosselin, 1988). Now, matrix $\mathbf{J}$ and the vector of generalized speeds $\dot{\boldsymbol{\theta}}$ are partitioned in such a way that eq.(12) can be expressed as

$$\mathbf{J}_I\dot{\boldsymbol{\theta}}_I + \mathbf{J}_D\dot{\boldsymbol{\theta}}_D = \mathbf{0} \tag{13}$$

where $\mathbf{J}_I$ and $\mathbf{J}_D$ are $m' \times n$ and $m' \times m$ matrices, respectively, whereas $\dot{\boldsymbol{\theta}}_I$ and $\dot{\boldsymbol{\theta}}_D$ are n- and m-dimensional vectors of *independent* and *dependent generalized speeds*, respectively. Moreover, if the machine is controllable by its minimal set of *actuated* joints, then $\mathbf{J}_D$ is of full rank and, in fact, it is a square matrix, i.e., $m' = m$. Hence, *dependent* joint rates can be evaluated from eq.(13) as

$$\dot{\boldsymbol{\theta}}_D = -\mathbf{J}_D^{-1}\mathbf{J}_I\dot{\boldsymbol{\theta}}_I \tag{14}$$

Furthermore, the *generalized twist* vector can be written as

$$\mathbf{t} = \mathbf{T}_I\dot{\boldsymbol{\theta}}_I + \mathbf{T}_D\dot{\boldsymbol{\theta}}_D \tag{15}$$

where $\mathbf{T}_I$ and $\mathbf{T}_D$ are $6l \times n$ and $6l \times m$ matrices, respectively. Upon substitution of eq.(14) into eq.(15) we obtain an expression for $\mathbf{t}$ as a linear transformation of $\dot{\boldsymbol{\theta}}_I$, namely,

$$\mathbf{t} = (\mathbf{T}_I - \mathbf{T}_D\mathbf{J}_D^{-1}\mathbf{J}_I)\dot{\boldsymbol{\theta}}_I$$

Since vector $\dot{\boldsymbol{\theta}}_I$ is defined as the vector of independent generalized speeds, *the natural orthogonal complement* matrix in the presence of unactuated joints is defined as

$$\mathbf{T} = \mathbf{T}_I - \mathbf{T}_D\mathbf{J}_D^{-1}\mathbf{J}_I \tag{16}$$

Then, matrix $\dot{\mathbf{T}}$, needed in eq.(10), is obtained as

$$\dot{\mathbf{T}} = \dot{\mathbf{T}}_I - \dot{\mathbf{T}}_D\mathbf{J}_D^{-1}\mathbf{J}_I + \mathbf{T}_D\mathbf{J}_D^{-1}\dot{\mathbf{J}}_D\mathbf{J}_D^{-1}\mathbf{J}_I - \mathbf{T}_D\mathbf{J}_D^{-1}\dot{\mathbf{J}}_I \tag{17}$$

It is evident from eqs.(16) and (17) that matrices $\mathbf{T}$ and $\dot{\mathbf{T}}$ are given by cumbersome expressions. For multi-kinematic-loop systems, an efficient method of calculating both $\mathbf{T}$ and $\dot{\mathbf{T}}$ numerically is reported in Saha and Angeles (1991). Knowing matrices $\mathbf{T}$ and $\dot{\mathbf{T}}$, the equations of motion for closed-loop mechanical systems are readily derived from eq.(11).

4 Dynamics of Planar Mechanisms

In this section the kinematic constraints and the equations of motion of several one-degree-of-freedom planar mechanisms are derived using the method presented in the previous sections. These mechanisms are chosen due to their significant importance and widespread applicability in industrial machinery. Note that, for the analysis of planar mechanisms, the *twist* $\mathbf{t}_i$ and the *wrench* $\mathbf{w}_i$ of the ith body, moving in a plane, are redefined as three-dimensional vectors. Moreover, the *extended mass* matrix $\mathbf{M}_i$ is redefined as a 3×3 matrix. They are given below:

$$\mathbf{t}_i = \begin{bmatrix} \omega_i \\ \dot{\mathbf{c}}_i \end{bmatrix}, \quad \mathbf{w}_i = \begin{bmatrix} n_i \\ \mathbf{f}_i \end{bmatrix}, \quad \text{and} \quad \mathbf{M}_i = \begin{bmatrix} I_i & \mathbf{O} \\ \mathbf{O} & m_i\mathbf{1} \end{bmatrix} \tag{18}$$

where ω_i, n_i and I_i are the scalar angular velocity of the ith link, applied scalar torque acting on the ith link and the—polar—mass moment of inertia of the ith link about its mass center, respectively. All these quantities are defined about an axis orthogonal to the plane of motion. Vectors $\dot{\mathbf{c}}_i$ and $\mathbf{f}_i$ are redefined as the two-dimensional vectors representing the velocity of the mass center and the resultant force acting at the mass center of the ith link, respectively. Moreover, $\mathbf{O}$ and $\mathbf{1}$ are now the 2×2 zero and identity matrices, respectively. Note that, in a plane, constraint torques and forces exerted by the ith link on the jth link through the (i, j) coupling will be denoted by a scalar n_{ij} and a two-dimensional vector $\mathbf{f}_{ij}$, respectively. Moreover, from the Third Law of Newton, n_{ij} and $\mathbf{f}_{ij}$ are equal to $-n_{ji}$ and $-\mathbf{f}_{ji}$, respectively.

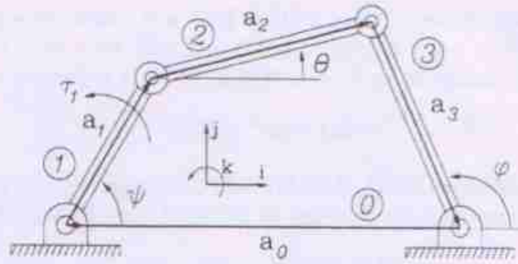

Fig. 1 A four-bar linkage

4.1 A Four-Bar Linkage

A planar linkage consisting of four rigid links coupled by revolute joints, as shown in Fig. 1, is among the simplest, yet the most important mechanisms. To derive the kinematic constraints of a four-bar linkage, note that the angular velocities are parallel to vector $\mathbf{k}$, as indicated in Fig. 1, and hence, constraint equations on angular velocities of the coupled bodies vanish identically, the constraint equations on mass-center velocities being derived as

$$\dot{\mathbf{c}}_i = \dot{\mathbf{c}}_{i-1} + \omega_{i-1}\mathbf{E}\mathbf{b}_{i-1} + \omega_i\mathbf{E}\mathbf{r}_i \tag{19}$$

where $\dot{\mathbf{c}}_{i-1}$ and $\dot{\mathbf{c}}_i$ denote the velocity of the mass center of the $(i-1)$st and the ith links, respectively. Therefore, the 2×3 matrices $\mathbf{A}_{i-1,i-1}$ and $\mathbf{A}_{i-1,i}$ for a revolute joint are

$$\mathbf{A}_{i-1,i-1} \equiv [-\mathbf{E}\mathbf{b}_{i-1} \quad -\mathbf{1}], \quad \mathbf{A}_{i-1,i} \equiv [-\mathbf{E}\mathbf{r}_i \quad \mathbf{1}] \tag{20}$$

where $\mathbf{b}_i \equiv \mathbf{a}_i - \mathbf{r}_i$, for $i = 0, 1, 2, 3$. Using eq.(20), the kinematic constraint matrix, introduced in eq.(6), is derived as

$$\mathbf{A} = \begin{bmatrix} -\mathbf{E}\mathbf{r}_1 & \mathbf{1} & \mathbf{0} & \mathbf{O} & \mathbf{0} & \mathbf{O} \\ -\mathbf{E}\mathbf{b}_1 & -\mathbf{1} & -\mathbf{E}\mathbf{r}_2 & \mathbf{1} & \mathbf{0} & \mathbf{O} \\ \mathbf{0} & \mathbf{O} & -\mathbf{E}\mathbf{b}_2 & -\mathbf{1} & -\mathbf{E}\mathbf{r}_3 & \mathbf{1} \\ \mathbf{0} & \mathbf{O} & \mathbf{0} & \mathbf{O} & -\mathbf{E}\mathbf{b}_3 & -\mathbf{1} \end{bmatrix} \tag{21}$$

where $\mathbf{A}$ is an 8×9 matrix, $\mathbf{O}$ was already introduced in eq.(18) and $\mathbf{0}$ is the 2-dimensional zero vector.

Now, from the free-body diagram of the ith link, shown in Fig. 1, the Newton-Euler equations of the ith link moving in a plane are given as

$$n_i + \mathbf{r}_i^T\mathbf{E}\mathbf{f}_{i-1,i} + (\mathbf{a}_i - \mathbf{r}_i)^T\mathbf{E}\mathbf{f}_{i,i+1} = I_i\dot{\omega}_i \tag{22}$$

$$\mathbf{f}_i + \mathbf{f}_{i-1,i} - \mathbf{f}_{i,i+1} = m_i\ddot{\mathbf{c}}_i \tag{23}$$

where $i = 1, 2, 3$. Moreover, the scalar n_i and the vector $\mathbf{f}_i$, included in Fig. 3(a), denote, respectively, the scalar moment and the 2-dimensional vector of applied force acting at the mass center of the link, C_i. Moreover, $\mathbf{E}$ is a 2×2 orthogonal matrix that rotates 2-dimensional vectors clockwise through an angle of 90°. It is defined as

$$\mathbf{E} \equiv \begin{bmatrix} 0 & -1 \\ 1 & 0 \end{bmatrix}$$

and hence, $E^T = -E$ and $E^T E = E E^T = 1$. As a consequence, then, $E^2 = -1$. Writing eqs.(22) and (23) for $i = 1, 2, 3$, an equation similar to eq.(5) is obtained, which is expressed as

$$M\dot{t} = w^W + Bf^C \tag{24}$$

where the term WMt of eq.(5) does not come into the picture. Furthermore, the 9×9 matrix of *extended mass* M is given by

$$M = \mathrm{diag}(M_1,\ M_2,\ M_3) \tag{25}$$

where vector t_i and matrix M_i, for $i = 1, 2, 3$, are defined in eq.(18), while the 9×8 matrix B is given below:

$$B = \begin{bmatrix} r_1^T E & b_1^T E & 0^T & 0^T \\ 1 & -1 & O & O \\ 0^T & r_2^T E & b_2^T E & 0^T \\ O & 1 & -1 & O \\ 0^T & 0^T & r_3^T E & b_3^T E \\ O & O & 1 & -1 \end{bmatrix} \tag{26}$$

where vector b_i, for $i = 1, 2, 3$, is introduced in eq.(20). Moreover, the 9-dimensional vector w^W and the 8-dimensional vector f^C are

$$w^W = [(w_1^W)^T,\ (w_2^W)^T,\ (w_3^W)^T]^T \text{ and } f^C = [f_{01}^T,\ f_{12}^T,\ f_{23}^T,\ f_{30}^T]^T \tag{27}$$

where $w_i^W \equiv [n_i,\ f_i^T]^T$, for $i = 1, 2, 3$. Note that, matrix B in eq.(26) is identical to the transpose of matrix A, as given in eq.(21), which shows, as pointed out in Section 3, that the non-working constraint wrench Bf^C, as in eq.(24), lies in the range of the transpose of A.

Now, the twists of the individual links are obtained as

$$t_1 = \dot{\psi}\begin{bmatrix} 1 \\ Er_1 \end{bmatrix}, \quad t_2 = \dot{\theta}\begin{bmatrix} 1 \\ Er_2 \end{bmatrix} \quad \text{and} \quad t_3 = \dot{\phi}\begin{bmatrix} 1 \\ Er_3 \end{bmatrix} \tag{28}$$

Since a four-bar linkage is a one-degree-of-freedom mechanical system, in order to find the generalized twist as a linear transformation of the independent joint rate $\dot{\psi}$, joint rates $\dot{\theta}$ and $\dot{\phi}$ have to be evaluated in terms of $\dot{\psi}$. This is done below: From Fig. 1,

$$a_1 + a_2 + a_3 + a_0 = 0 \tag{29}$$

Upon differentiation of eq.(29) with respect to time, a relation, similar to eq.(13), is obtained as

$$h\dot{\psi} + J_D \dot{\theta}_D = 0 \tag{30}$$

where the 2-dimensional vector h and the 2×2 matrix, J_D are given as

$$h = -Ea_1, \qquad J_D = [Ea_2,\ Ea_3]$$

and $\dot{\theta}_D \equiv [\dot{\theta},\ \dot{\phi}]^T$. Moreover, for nonparallel vectors a_2 and a_3, J_D is nonsingular. Hence, $\dot{\theta}$ and $\dot{\phi}$ are obtained from eq.(30) as

$$\dot{\theta} = r_\theta \dot{\psi}, \qquad \dot{\phi} = r_\phi \dot{\psi} \tag{31}$$

where r_θ and r_ϕ are evaluated as $[r_\theta,\ r_\phi]^T = -J_D^{-1} h$. Furthermore, the four-bar linkage is in a singular configuration when matrix J_D is singular, i.e., a_2 and a_3 are parallel, that is, at the dead points of the output link.

Knowing $\dot{\theta}$ and $\dot{\phi}$, the 9-dimensional *generalized twist* can be expressed as

$$t = u\dot{\psi}$$

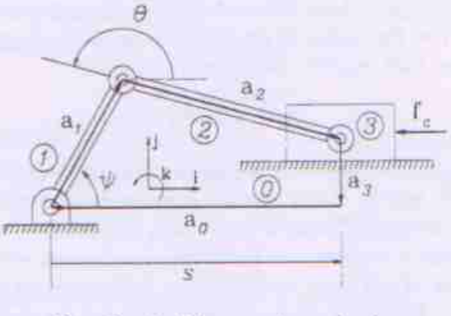

Fig. 2 A slider-crank mechanism

where *the natural orthogonal complement* of matrix A, as given in eq.(21), is now vector u displayed below:

$$u = [1,\ -r_1^T E,\ r_\theta,\ -(a_1 + r_\theta r_2)^T E,\ r_\phi,\ r_\phi b_1^T E]^T$$

Now, using eq.(30), it can be readily seen that

$$Au = 0$$

The generalized inertia and convective inertia terms, denoted by scalars I and C, respectively, for a four-bar linkage, are given as

$$\begin{aligned} I &= I_1 + r_\theta^2 I_2 + r_\phi^2 I_3 + m_1\|r_1\|^2 + m_2\|a_1 + r_\theta r_2\|^2 \\ &\quad + m_3 r_\phi^2 \|b_3\|^2 \end{aligned} \tag{32}$$

$$\begin{aligned} C &= -\dot{\psi}[r_\theta r_\theta'(I_2 + m_2\|r_2\|^2) + m_2 r_\theta' a_1^T r_2 \\ &\quad + m_2 r_\theta (r_\theta - 1) a_1^T E r_2 + r_\phi r_\phi' (I_3 + m_3\|b_3\|^2)] \end{aligned} \tag{33}$$

where $\|\cdot\|$ denotes the Euclidean norm of a vector $(\cdot)$, whereas $(\cdot)'$ is $d(\cdot)/d\psi$. Furthermore, if the mechanism is assumed to lie in a vertical plane, then the gravity acceleration, denoted by vector g, acts along $-j$, while a driving torque τ_1 is assumed to be applied on link 1. Therefore, the scalar external generalized torque, τ is given as

$$\tau = \tau_1 - g^T E[m_1 r_1 + m_2(a_1 + r_\theta r_2) - m_3 r_\phi b_3] + \tau^D \tag{34}$$

where torque τ^D arises from the dissipation effects in the system. Finally, the equation of motion of a four-bar linkage is obtained as

$$I\ddot{\psi} = C\dot{\psi} + \tau \tag{35}$$

where I, C and τ are evaluated form eqs.(32), (33) and (34), respectively.

4.2 A Slider-Crank Mechanism

A slider-crank mechanism is shown in Fig. 2. The kinematic constraints between links 0 and 1, 1 and 2, and 2 and 3 can be readily derived using eq.(19). To derive constraints between the slider and the fixed base, links 3 and 0, respectively, it is noted that link 3 has only translational motion along vector i. Thus, this constraint can be expressed as

$$\omega_3 = 0 \quad \text{and} \quad j^T \dot{c}_3 = 0 \tag{36}$$

Combining eq.(36) with other constraints and writing them in the form of eq.(6), the 8×9 matrix A is obtained as shown below:

$$A = \begin{bmatrix} -Er_1 & 1 & 0 & O & 0 & O \\ -Eb_1 & -1 & -Er_2 & 1 & 0 & O \\ 0 & O & -Eb_2 & -1 & -Er_3 & 1 \\ 0 & 0^T & 0 & 0^T & -1 & 0 \\ 0 & 0^T & 0 & 0^T & 0 & -j^T \end{bmatrix} \tag{37}$$

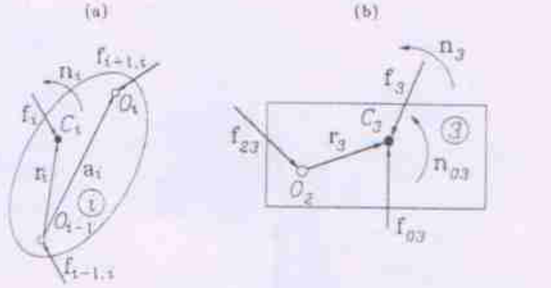

Fig. 3 Free-body diagrams of (a) a link and (b) a slider.

where $\mathbf{1}$, $\mathbf{O}$ and $\mathbf{0}$ were defined in Subsection 4.1. The free-body diagram of the slider is shown in Fig. 3(b). Note that, in order to account for the offset of the point of application of the reaction force, $\mathbf{f}_{03}$, it is assumed that link 0 exerts on link 3 a force $\mathbf{f}_{03}$ acting at C_3 and a couple n_{03}. From Fig. 3(b), the Newton-Euler equations are written as

$$n_3 + \mathbf{r}_3^T\mathbf{E}\mathbf{f}_{23} - n_{30} = 0 \tag{38}$$

$$\mathbf{f}_3 + \mathbf{f}_{23} - \mathbf{f}_{30} = m_3\ddot{\mathbf{c}}_3 \tag{39}$$

Using eqs.(22) and (23) for links 1 and 2, a set of dynamics equations in the form of eq.(24) is obtained where, for the slider-crank mechanism, the 9×9 extended mass matrix $\mathbf{M}$ is defined in eq.(25). Matrix $\mathbf{M}_i$, for $i = 1, 2$, is defined in eq.(18) and $\mathbf{M}_3$ is given as

$$\mathbf{M}_3 \equiv \begin{bmatrix} 0 & 0 \\ \mathbf{O} & m_3\mathbf{1} \end{bmatrix} \tag{40}$$

Moreover, vector $\mathbf{w}^W$ is defined as in eq.(27). Now, the 9×8 matrix $\mathbf{B}$ is given as

$$\mathbf{B} = \begin{bmatrix} \mathbf{r}_1^T\mathbf{E} & \mathbf{b}_1^T\mathbf{E} & \mathbf{0}^T & 0 & 0 \\ \mathbf{1} & -\mathbf{1} & \mathbf{O} & \mathbf{0} & \mathbf{0} \\ \mathbf{0}^T & \mathbf{r}_2^T\mathbf{E} & \mathbf{b}_2^T\mathbf{E} & 0 & 0 \\ \mathbf{O} & \mathbf{1} & -\mathbf{1} & \mathbf{0} & \mathbf{0} \\ \mathbf{0}^T & \mathbf{0}^T & \mathbf{r}_3^T\mathbf{E} & -1 & 0 \\ \mathbf{O} & \mathbf{O} & \mathbf{1} & \mathbf{0} & -\mathbf{j} \end{bmatrix} \tag{41}$$

while $\mathbf{f}^C$ is

$$\mathbf{f}^C = [\mathbf{f}_{01}^T,\ \mathbf{f}_{12}^T,\ \mathbf{f}_{23}^T,\ n_{30},\ f_{30}]^T$$

where $f_{30} = \mathbf{j}^T\mathbf{f}_{30}$. Also note that, upon comparison of eqs.(37) and (41), $\mathbf{B} = \mathbf{A}^T$ again. Furthermore, the twist of links 1 and 2 are given in eq.(28), whereas the twist of link 3 is

$$\mathbf{t}_3 = [0,\ -\dot{s}\mathbf{i}^T]^T$$

Now, the dependent variables $\dot{\theta}$ and $\dot{s}$ are obtained from Fig. 2 using eq.(29). Upon differentiation of eq.(29) with respect to time, an expression similar to eq.(30) is derived, where the 2-dimensional vector $\mathbf{h}$ and the 2×2 non-singular matrix $\mathbf{J}_D$ are given as

$$\mathbf{h} = -\mathbf{E}\mathbf{a}_1, \qquad \mathbf{J}_D = [\mathbf{E}\mathbf{a}_2,\ -\mathbf{i}] \tag{42}$$

Moreover, $\boldsymbol{\theta}_D \equiv [\theta,\ s]^T$. Then, $\dot{\theta}$ and $\dot{s}$ are obtained, similar to eq.(31), as $r_\theta\dot{\psi}$ and $r_s\dot{\psi}$, respectively. The 9-dimensional natural orthogonal complement of $\mathbf{A}$, as given in eq.(37), is now obtained as

$$\mathbf{u} = [1,\ -\mathbf{r}_1^T\mathbf{E},\ r_\theta,\ -(\mathbf{a}_1 + r_\theta\mathbf{r}_2)^T\mathbf{E},\ 0,\ r_s\mathbf{i}^T]^T$$

which satisfies $\mathbf{A}\mathbf{u} = \mathbf{0}$.

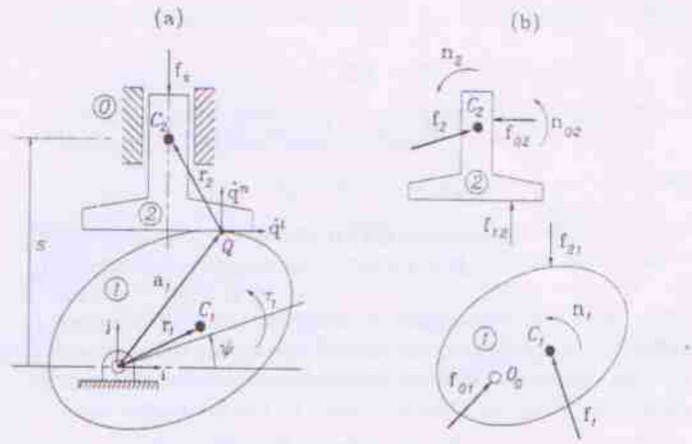

Fig. 4 (a) A cam with a flat-face follower, (b) Free-body diagram of the cam and the follower.

The generalized inertia, convective inertia and generalized torque in the presence of gravity, dissipation and external applied force $\mathbf{f}_c$—e.g., a compressive force in the cylinder of an internal combustion engine—applied on the slider, as shown in Fig. 2, are given as

$$I = I_1 + m_1\|\mathbf{r}_1\|^2 + r_\theta^2 I_2 + m_2\|\mathbf{a}_1 + r_\theta\mathbf{r}_2\|^2 + m_3 r_s^2 \tag{43}$$

$$C = -\dot{\psi}[I_2 r_\theta r_\theta' + m_2\{r_\theta'(\mathbf{a}_1 + r_\theta\mathbf{r}_2)^T\mathbf{r}_2 + r_\theta(r_\theta - 1)\mathbf{a}_1^T\mathbf{E}\mathbf{r}_2\} + m_3 r_s r_s'] \tag{44}$$

$$\tau = -\mathbf{g}^T\mathbf{E}[m_1\mathbf{r}_1 + m_2(\mathbf{a}_1 + r_\theta\mathbf{r}_2)] - r_s f_c + \tau^D \tag{45}$$

where $f_c = -\mathbf{i}^T\mathbf{f}_c$ and τ^D is the dissipation torque. Now the equation of motion of a slider-crank mechanism, as shown in eq.(35), is complete, I, C and τ being obtained from eqs.(43), (44) and (45), respectively.

4.3 A Flat-Face Follower Cam Mechanism

A cam mechanism with a flat-face follower is shown in Fig. 4(a). Constraint equations due to a revolute and a prismatic pair were derived in Subsections 4.1 and 4.2. Here, constraints between the cam and the flat-face follower are derived to obtain the constraint equations of the system under study. Note that, as shown in Fig. 4(a), the velocity of the contact point Q, regarded as a point of the cam, has a component parallel to $\mathbf{i}$ and a component parallel to $\mathbf{j}$, labeled $\dot{\mathbf{q}}^t$ and $\dot{\mathbf{q}}^n$, as shown in Fig. 4(a), respectively. Therefore, the velocity of the mass center of the follower can be written as

$$\dot{\mathbf{c}}_2 = \mathbf{j}^T[\dot{\mathbf{c}}_1 + \omega_1\mathbf{E}\mathbf{b}_1 + \omega_2\mathbf{E}\mathbf{r}_2]\mathbf{j} \tag{46}$$

Vector $\mathbf{b}_1$ is defined, as in Subsections 4.1 and 4.2, as $\mathbf{b}_1 \equiv \mathbf{a}_1 - \mathbf{r}_1$, while vectors $\mathbf{a}_1$ and $\mathbf{r}_1$ are shown in Fig. 4(a). Using eqs.(20), (36) and (46), the 6×6 matrix $\mathbf{A}$ for the mechanism at hand is derived as

$$\mathbf{A} = \begin{bmatrix} -\mathbf{E}\mathbf{r}_1 & \mathbf{1} & \mathbf{0} & \mathbf{O} \\ -(\mathbf{j}^T\mathbf{E}\mathbf{b}_1)\mathbf{j} & -\mathbf{j}\mathbf{j}^T & -(\mathbf{j}^T\mathbf{E}\mathbf{r}_2)\mathbf{j} & \mathbf{1} \\ 0 & \mathbf{0}^T & -1 & \mathbf{0}^T \\ 0 & \mathbf{0}^T & 0 & -\mathbf{i}^T \end{bmatrix} \tag{47}$$

From the free-body diagrams of the cam and the follower, as shown in Fig 4(b), the Newton-Euler equations for the cam and the follower are written as

$$n_1 + \mathbf{r}_1^T\mathbf{E}\mathbf{f}_{01} + \mathbf{b}_1^T\mathbf{E}\mathbf{f}_{12} = I_1\dot{\omega}_1 \tag{48}$$

$$\mathbf{f}_1 + \mathbf{f}_{01} - \mathbf{f}_{12} = m_1\ddot{\mathbf{c}}_1 \quad (49)$$

and

$$n_2 - n_{20} + \mathbf{r}_2^T\mathbf{E}\mathbf{f}_{12} = 0 \quad (50)$$
$$\mathbf{f}_2 - f_{20}\mathbf{i} + \mathbf{f}_{12} = m_2\ddot{\mathbf{c}}_2 \quad (51)$$

where $f_{20} = \mathbf{i}^T\mathbf{f}_{20}$. Note that the constraint force $\mathbf{f}_{12}$ acts along $\mathbf{j}$, and is the component of the force $\boldsymbol{\lambda}$ exerted by the cam on the follower. Vector $\boldsymbol{\lambda}$ can be interpreted as the vector of Lagrange multipliers. Now, the constraint force $\mathbf{f}_{12}$ can be written as

$$\mathbf{f}_{12} = (\mathbf{j}^T\boldsymbol{\lambda})\mathbf{j} \quad (52)$$

Moreover, as pointed out in the previous subsection, due to the offset of the point of application of force $\mathbf{f}_{02}$, a force $\mathbf{f}_{02}$ acting on the mass center of the follower and a couple n_{02} acting on the follower, as shown in Fig. 4(b), are included. Upon substitution of eq.(52) into eqs.(48) to (51), the governing equation in the form of eq.(24) can be written for the mechanism, where the 6×6 matrix $\mathbf{M}$ is defined similar to eq.(25), but the definitions of $\mathbf{M}_1$ and $\mathbf{M}_2$ are given in eqs.(18) and (40), respectively. Moreover, the 6×6 matrix $\mathbf{B}$ and the 6-dimensional vector $\mathbf{f}^C$ are given below:

$$\mathbf{B} = \begin{bmatrix} \mathbf{r}_1^T\mathbf{E} & (\mathbf{b}_1^T\mathbf{E}\mathbf{j})\mathbf{j}^T & 0 & 0 \\ 1 & -\mathbf{j}\mathbf{j}^T & 0 & 0 \\ \mathbf{0}^T & (\mathbf{r}_2^T\mathbf{E}\mathbf{j})\mathbf{j}^T & -1 & 0 \\ \mathbf{O} & 1 & 0 & -\mathbf{i} \end{bmatrix} \quad \text{and} \quad \mathbf{f}^C = \begin{bmatrix} \mathbf{f}_{01} \\ \boldsymbol{\lambda} \\ n_{20} \\ f_{20} \end{bmatrix} \quad (53)$$

from which it is clear that, again, $\mathbf{B}=\mathbf{A}^T$. The twist $\mathbf{t}_1$ of the cam is obtained from eq.(28), whereas the twist of the follower, $\mathbf{t}_2$, is given by $[0, \ \dot{s}\mathbf{j}^T]^T$, where

$$\dot{s} = (\mathbf{j}^T\mathbf{E}\mathbf{a}_1)\dot{\psi}$$

Now, the natural orthogonal complement reduces to a 6-dimensional vector $\mathbf{u}$ that is given as

$$\mathbf{u} = [1, \ -\mathbf{r}_1^T\mathbf{E}, \ 0, \ -(\mathbf{a}_1^T\mathbf{E}\mathbf{j})\mathbf{j}^T]^T$$

Moreover, with a driving motor torque τ_1 on the cam and an external force $\mathbf{f}_s$ acting on the follower, as shown in Fig. 4(b), the equation of motion of this mechanism can be obtained, as in eq.(35), with I, C and τ given below:

$$\begin{aligned} I &= I_1 + m_1\|\mathbf{r}_1\|^2 + m_2(\mathbf{i}^T\mathbf{a}_1)^2 \\ C &= \dot{\psi}[m_1\|\mathbf{r}_1\|^2 - m_2(\mathbf{i}^T\mathbf{a}_1)(\mathbf{j}^T\mathbf{a}_1)] \\ \tau &= \tau_1 + m_1\mathbf{r}_1^T\mathbf{E}\mathbf{g} - (\mathbf{i}^T\mathbf{a}_1)[m_2(\mathbf{j}^T\mathbf{g}) + f_s] + \tau^D \end{aligned}$$

where $f_s = -\mathbf{j}^T\mathbf{f}_s$. Furthermore, vector $\mathbf{g}$ and scalar τ^D denote the gravity acceleration and the dissipation torque, respectively.

4.4 A Roller-Follower Cam Mechanism

Referring to Fig. 5, the constraint equation due to the rolling contact between the cam and the roller-follower is written in the form of eq.(19), which, when combined with other constraints, yields the 8×9 matrix $\mathbf{A}$ shown below:

$$\mathbf{A} = \begin{bmatrix} -\mathbf{E}\mathbf{r}_1 & 1 & 0 & \mathbf{O} & 0 & \mathbf{O} \\ -\mathbf{E}\mathbf{b}_1 & -1 & -\mathbf{E}\mathbf{r}_2 & 1 & 0 & \mathbf{O} \\ 0 & \mathbf{O} & 0 & -1 & -\mathbf{E}\mathbf{r}_3 & 1 \\ 0 & \mathbf{0}^T & 0 & \mathbf{0}^T & -1 & \mathbf{0}^T \\ 0 & \mathbf{0}^T & 0 & \mathbf{0}^T & 0 & -\mathbf{i}^T \end{bmatrix} \quad (54)$$

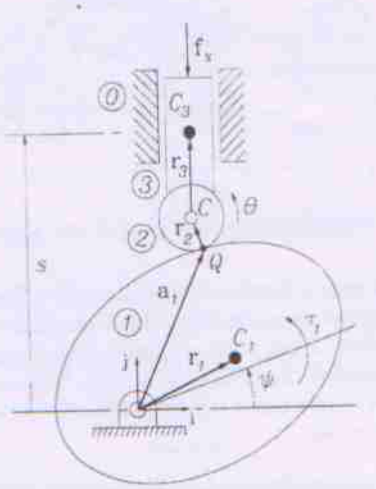

Fig. 5 A cam with a roller follower.

The Newton-Euler equations for the cam and the roller can be written as in eqs.(22) and (23), whereas the dynamics equations for the follower, link 3, can be obtained as in the previous subsection. This results in a set of equations of motion of the form shown in eq.(24). The 9-dimensional vectors of generalized twist $\mathbf{t}$ and of generalized working wrench $\mathbf{w}^W$, as well as the 9×9 matrix of generalized mass, are as defined for the slider-crank mechanism. The 9×8 matrix $\mathbf{B}$ and the 8-dimensional vector $\mathbf{f}^C$ are given as

$$\mathbf{B} = \begin{bmatrix} \mathbf{r}_1^T\mathbf{E} & \mathbf{b}_1^T\mathbf{E} & \mathbf{0}^T & 0 & 0 \\ 1 & -1 & \mathbf{O} & 0 & 0 \\ \mathbf{0}^T & \mathbf{r}_2^T\mathbf{E} & \mathbf{0}^T & 0 & 0 \\ \mathbf{O} & 1 & -1 & 0 & 0 \\ \mathbf{0}^T & \mathbf{0}^T & \mathbf{r}_3^T\mathbf{E} & -1 & 0 \\ \mathbf{O} & \mathbf{O} & 1 & 0 & -\mathbf{i} \end{bmatrix} \quad \text{and} \quad \mathbf{f}^C = \begin{bmatrix} \mathbf{f}_{01} \\ \mathbf{f}_{12} \\ \mathbf{f}_{23} \\ n_{30} \\ f_{30} \end{bmatrix} \quad (55)$$

where n_{30} arises due to the offset of the point of application of force $\mathbf{f}_{30}$. Moreover, f_{30} is the component of the force $\mathbf{f}_{30}$ along $-\mathbf{i}$. Note that, as in previous cases, $\mathbf{A} = \mathbf{B}^T$.

For the roller-follower cam mechanism, the angular rate of the roller $\dot{\theta}$ and the sliding rate $\dot{s}$ are dependent variables. They are computed from the constraints arising from the rolling contact between the cam and the roller, which can be expressed as

$$\dot{s}\mathbf{j} + \dot{\theta}\mathbf{E}\mathbf{r}_2 = \dot{\psi}\mathbf{E}\mathbf{a}_1$$

Now, the natural orthogonal complement is a 9-dimensional vector $\mathbf{u}$, namely,

$$\mathbf{u} = [1, \ -\mathbf{r}_1^T\mathbf{E}, \ -r_\theta, \ r_s\mathbf{j}^T, \ 0, \ r_s\mathbf{j}^T]^T$$

Therefore, I, C and τ for the dynamical equation of this mechanism are given as

$$\begin{aligned} I &= I_1 + m_1\|\mathbf{r}_1\|^2 + I_2 r_\theta^2 + (m_2 + m_3)r_s^2 \\ C &= -\dot{\psi}[I_2 r_\theta r'_\theta + (m_2 + m_3)r_s r'_s] \\ \tau &= \tau_1 + m_1\mathbf{r}_1^T\mathbf{E}\mathbf{g} - r_s[(m_2 + m_3)(\mathbf{j}^T\mathbf{g}) + f_s] + \tau^D \end{aligned}$$

where τ_1 is a driving torque acting on the cam and f_s is the component of the external force, acting on follower, along $-\mathbf{j}$, as shown in Fig. 5. Moreover, τ^D is the torque arising from the dissipation in the system.

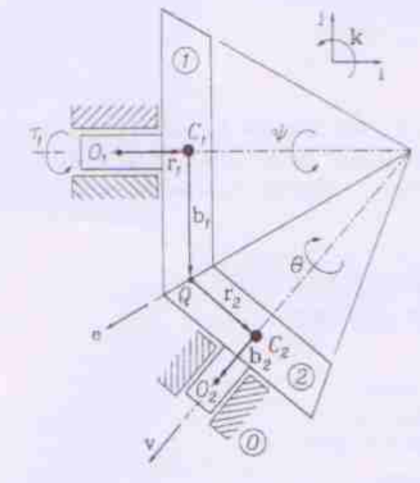

Fig. 6 A bevel gear train.

5 A Bevel Gear Train

Referring to Fig. 6, Q is the contact point between the bevel gears, links 1 and 2. Moreover, the orthonormal vectors $\mathbf{i}$, $\mathbf{j}$ and $\mathbf{k}$ are shown in Fig. 6. Furthermore, we define the unit vector $\mathbf{e}$ in the direction of the common element of the two conic pitch surfaces of the bevel gears, whereas vector $\mathbf{v}$ is parallel to the axis of rotation of link 2. Note that, for the gear train under study, the definitions of vectors and matrices in a plane, as in Section 4, are not sufficient, as the angular velocities of the gears are not parallel. Therefore, the definitions introduced in Sections 2 and 3 are used here. Now, the constraint equations for the two mating bevel gears, links 1 and 2, are readily derived, namely,

$$\mathbf{A}_{11}\mathbf{t}_1 + \mathbf{A}_{12}\mathbf{t}_2 = \mathbf{0} \tag{56}$$

the 6×6 coefficient matrices being given by

$$\mathbf{A}_{11} = \begin{bmatrix} -\mathbf{F} & \mathbf{O} \\ \mathbf{B}_1 & -\mathbf{1} \end{bmatrix}, \qquad \mathbf{A}_{12} = \begin{bmatrix} \mathbf{F} & \mathbf{O} \\ \mathbf{R}_2 & \mathbf{1} \end{bmatrix}$$

where $\mathbf{F}$, $\mathbf{B}_1$ and $\mathbf{R}_2$ are the *cross-product* matrices, as defined in eq.(2) for vector $\boldsymbol{\omega}$, associated with vectors $\mathbf{e}$, $\mathbf{b}_1$ and $\mathbf{r}_2$, respectively, as shown in Fig. 6. Combining eq.(56) with constraints arising at the revolute joints O_1 and O_2, the 18×12 matrix $\mathbf{A}$ is obtained as

$$\mathbf{A} = \begin{bmatrix} \mathbf{L} & \mathbf{O} & \mathbf{O} & \mathbf{O} \\ \mathbf{R}_1 & \mathbf{1} & \mathbf{O} & \mathbf{O} \\ -\mathbf{F} & \mathbf{O} & \mathbf{F} & \mathbf{O} \\ \mathbf{B}_1 & -\mathbf{1} & \mathbf{R}_2 & \mathbf{1} \\ \mathbf{O} & \mathbf{O} & -\mathbf{V} & \mathbf{O} \\ \mathbf{O} & \mathbf{O} & \mathbf{B}_2 & -\mathbf{1} \end{bmatrix} \tag{57}$$

where $\mathbf{L}$, $\mathbf{R}_1$, $\mathbf{B}_2$ and $\mathbf{V}$ are the *cross-product* matrices derived from vectors $\mathbf{i}$, $\mathbf{r}_1$, $\mathbf{b}_2$ and $\mathbf{v}$, respectively.

The Newton-Euler equations of link 1, shown in Fig. 6, can be written as

$$\mathbf{n}_1 + \mathbf{n}_{01} + \mathbf{f}_{01} \times \mathbf{r}_1 - \mathbf{n}_{12} + \mathbf{f}_{12} \times \mathbf{b}_1 = \mathbf{I}_1\dot{\boldsymbol{\omega}}_1 \tag{58}$$

$$\mathbf{f}_1 + \mathbf{f}_{01} - \mathbf{f}_{12} = m_1\ddot{\mathbf{c}}_1 \tag{59}$$

To find an expression for the constraint moment $\mathbf{n}_{01}$ for a revolute joint, O_1, it is noted that an applied torque $\boldsymbol{\tau}_{01}$ at joint O_1 consists of two components, namely,

$$\boldsymbol{\tau}_{01} = \mathbf{n}_{01} + \boldsymbol{\tau}_1$$

where, $\boldsymbol{\tau}_1$ lies in the direction of $\mathbf{i}$ and $\mathbf{n}_{01}$ is perpendicular to $\mathbf{i}$, i.e.,

$$\mathbf{L}\boldsymbol{\tau}_1 = \mathbf{0}$$

while $\mathbf{n}_{01}$ can be written as the mapping of a certain vector $\boldsymbol{\lambda}_{01}$ by matrix $\mathbf{L}^T$ defined above, namely,

$$\mathbf{n}_{01} = \mathbf{L}^T\boldsymbol{\lambda}_{01} = -\mathbf{L}\boldsymbol{\lambda}_{01} \tag{60}$$

where $\boldsymbol{\lambda}_{01}$ plays the role of a vector of Lagrange multipliers. Upon substitution of eq.(60) into eq.(58), and with similar calculations for other joints Q and O_2, an equation similar to eq.(21) is obtained, where $\mathbf{M}$ is a 12×12 matrix and $\mathbf{t}$ and $\mathbf{w}^W$ are 12-dimensional vectors. Moreover, the 12×18 matrix $\mathbf{B}$ and the 18-dimensional vector of constraint force $\mathbf{f}^C$ are written as

$$\mathbf{B} = \begin{bmatrix} -\mathbf{L} & -\mathbf{R}_1 & \mathbf{F} & -\mathbf{B}_1 & \mathbf{O} & \mathbf{O} \\ \mathbf{O} & \mathbf{1} & \mathbf{O} & -\mathbf{1} & \mathbf{O} & \mathbf{O} \\ \mathbf{O} & \mathbf{O} & -\mathbf{F} & -\mathbf{R}_2 & \mathbf{V} & -\mathbf{B}_2 \\ \mathbf{O} & \mathbf{O} & \mathbf{O} & \mathbf{1} & \mathbf{O} & -\mathbf{1} \end{bmatrix} \quad \text{and} \quad \mathbf{f}^C = \begin{bmatrix} \boldsymbol{\lambda}_{01} \\ \mathbf{f}_{01} \\ \boldsymbol{\lambda}_{12} \\ \mathbf{f}_{12} \\ \boldsymbol{\lambda}_{20} \\ \mathbf{f}_{20} \end{bmatrix} \tag{61}$$

Comparing eqs.(57) and (61), $\mathbf{A} = \mathbf{B}^T$, as expected.

Now, the twist of the individual gears can be written as

$$\mathbf{t}_1 = \dot{\psi}\begin{bmatrix} \mathbf{i} \\ \mathbf{0} \end{bmatrix}, \qquad \mathbf{t}_2 = \dot{\theta}\begin{bmatrix} \mathbf{v} \\ \mathbf{0} \end{bmatrix} \tag{62}$$

Note that this is a one-degree-of-freedom mechanical system, $\dot{\psi}$ and $\dot{\theta}$ being regarded as the *independent* and the *dependent* joint rates, respectively. Moreover, the constraint at the contact point of the gears is the velocity of Q, regarded as a point of link 1, is equal to the velocity of Q, when regarded as a point of link 2. This can be expressed as

$$\boldsymbol{\omega}_1 \times \mathbf{b}_1 = -\boldsymbol{\omega}_2 \times \mathbf{r}_2$$

which leads to

$$\dot{\theta} = -\frac{d_1}{d_2}\dot{\psi} \tag{63}$$

where d_1 and d_2 are the pitch circle diameters of gears 1 and 2, respectively. Upon substitution of eq.(63) into eq.(62), the natural orthogonal complement reduces to a 12-dimensional vector $\mathbf{u}$, which is written as

$$\mathbf{u} = [\mathbf{i}^T,\ \mathbf{0}^T,\ -(d_1/d_2)\mathbf{v}^T,\ \mathbf{0}^T]^T \tag{64}$$

It is evident from eq.(64) that the time rate of change of the natural orthogonal complement vector $\mathbf{u}$ vanishes. Therefore, the equation of motion of the gear train can be obtained from eq.(11), where the scalar quantity C vanishes and the resulting equation takes on the simple form

$$I\ddot{\psi} = \tau \tag{65}$$

with I and τ being given by

$$I = I_1 + (d_1/d_2)^2 I_2$$
$$\tau = \tau_1 + \tau^D$$

while I_1, I_2, τ_1 and τ^D are the mass moments of inertia of gears 1 and 2 about their axes of rotation, the applied torque about an axis parallel to $\mathbf{i}$ and the dissipation torque, respectively. These are rather standard results, but are included here because they constitute the building blocks for the modeling of more complex systems like differential gear trains.

6 Conclusions

It is apparent that kinematic constraints pertaining to machines can be written in the form of a system of linear homogeneous equations involving the twists of every pair of coupled links of the machine. The approach introduced here departs from that reported in the literature of deriving independent scalar constraint equations that are linear in the link twists, but not necessarily homogeneous. In fact, the homogeneity of those constraint equations allows us to regard all constraints as scleronomic. Moreover, the formulation of the kinematic constraints helps in finding the constraint forces, as constraint forces lie in the range of the transpose of the kinematic constraint matrix **A**. Contrary to simulation studies, in which no constraint forces are needed, these forces must be determined in designing machine elements. In fact, the kinematic constraints allow the calculation of non-working constraint forces and moments, i.e., wrenches, systematically. The duality between kinematic constraints and non-working constraint wrenches was fully exploited.

7 Acknowledgements

The research work reported here was possible under NSERC (Natural Sciences and Engineering Research Council, of Canada) Research Grant No. A4532 and Equipment Grant No. EQP00-92729. Partial support from the Institute for Robotics and Intelligent Systems, a network of Canadian centres of excellence, is highly acknowledged. The scholarship granted to Subir Kumar Saha by the Government of India is equally acknowledged.

8 References

Angeles, J., and Lee, S., 1988, "The formulation of dynamical equations of holonomic mechanical systems using a natural orthogonal complement," *Trans. of the ASME, J. of Applied Mechanics*Vol. 55, March, pp. 243–244.

Angeles, J., and Ma, O., 1988, "Dynamic simulation of n-axis serial robotic manipulators using a natural orthogonal complement," *The Int. J. of Robotics Research*, Vol. 7, No.5, pp. 32–47.

Cyril, X., Angeles, J. and Misra, A.K., 1989, "Flexible-link robotic manipulator dynamics," Proc. 1989 *American Control Conference*, Pittsburgh, June 21–23, pp. 2346–2351.

Huston, R.L., and Passerello, C.E., 1974, "On Constraint Equations—A New Approach," *Trans. of the ASME, J. of Applied Mechanics*, Vol. 41, December, pp. 1130–1131.

Gosselin, C., 1988, *Kinematic analysis, optimization and programming of parallel robotic manipulators*, Ph.D. Thesis, Dept. of Mech. Eng., McGill University, Canada.

Kane, T.R., and Wang, C.F., 1965, "On the derivation of equations of motion," *J. Soc. Indust. Appl. Math.*, Vol. 13, No. 2, pp. 487–492.

Meirovitch, L., 1970, *Methods of Analytical Dynamics*, McGraw-Hill, New York.

Saha, S.K. and Angeles, J., 1991 "Dynamics of nonholonomic mechanical systems using a natural orthogonal complement," *Trans. of the ASME, J. of Applied Mechanics*, Vol. 58, March, pp. 238–243.

Saha, S. K., and Angeles, J., 1989, "Kinematics and dynamics of 3-wheeled 2-DOF AGV," *Proc. of the IEEE Conf. on Robotics & Automation*, Scottsdale, Arizona, May, 14–19, pp. 1572–1577.